



An Adaptive Region Growing Method to Segment Inferior Alveolar Nerve Canal from 3D Medical Images for Dental Implant Surgery

H. T. Yau¹, Y. K. Lin², L. S. Tsou³ and C. Y. Lee⁴

¹ National Chung Cheng University, imehty@ccu.edu.tw

² National Chung Cheng University, arb1130@cad.me.ccu.edu.tw

³ National Chung Cheng University, ltsou@cad.me.ccu.edu.tw

⁴ National Chung Cheng University, leechanyo@cad.me.ccu.edu.tw

ABSTRACT

In implant surgeries, dentists need to consider the depth and angle of the fixture and density around the bone. Dentists must also consider the distance between the fixture and the inferior alveolar nerve canal. If the distance to a nerve is not taken into account, serious injury may result, leading to medical problems. Therefore, we use a method that automatically or semi-automatically finds nerves in computed tomography images. This method can help dentists find the inferior alveolar nerve canal before implant surgery, thereby reducing the risk of injury to patients. This research concerns the application of the seeded region growing method. We segment the inferior alveolar nerve canal from computed tomography images and show it in three dimensions. This will help dentists find the inferior alveolar nerve canal when they plan for implant surgery.

Keywords: Region Growing Method, Computed Tomography, Inferior Alveolar Nerve Canal.

DOI: 10.3722/cadaps.2008.743-752

1. INTRODUCTION

It has been more than 100 years since Rontgen first discovered the use of x-rays in 1895. Specifically, he found out that the medical imaging can play an important role in the diagnosis of illnesses. With the use of x-rays, the skeletal system within the human body can be viewed. The quality of the image will greatly influence the diagnosis.

Computed tomography (CT) is a medical imaging method that employs tomography in which digital geometry processing is used to generate a three-dimensional image of the inside of an object from a series of two-dimensional x-ray images taken around a single axis of rotation.

CT is more advantageous than projection radiography for a number of reasons: First, CT completely eliminates the superimposition of images of structures outside the area of interest. Second, because of the inherent high-contrast resolution of CT, differences between tissues that differ in physical density by less than 1% can be distinguished. Third, data from a single CT imaging procedure consisting of either multiple contiguous or one helical scan can be viewed as images in the axial, coronal, or sagittal planes, depending on the diagnostic task. This is referred to as multi-planar reformatted imaging. It makes it possible to assist dentists in further diagnosis of the body of his patients, for example, tissue damage, fractures, intra-cranial hemorrhaging and so on.

The method of CT reconstruction is a series of mathematical computations, so the different algorithms used to compute CT reconstruction influence the quality of the image. Good quality CT images help dentists make correct diagnoses. The applications of CT are extensive, including CT imaging of hard tissue within the human body, such as bones, teeth, and so on. In this paper, our work is concerned with CT imaging of the mandible.

Before the implant surgeries, dentists usually need an accurate preoperative planning which increases the dentist's confidence. A good preoperative planning focuses on the ideal positions of the implant fixtures. Because nerve canals are within the mandible, dentists must also consider the distance between the fixture and the nerve canal in the preoperative planning. In practice, the minimum safety distance is 2mm. If the distance to a nerve is not taken into

account, serious injury may result, leading to medical problems. When these nerve canals are highlighted in the preoperative planning, it is easier to take them into account. With medical imaging and image processing technology, the inferior alveolar nerve canal can be segmented from CT to help dentists avoid mistakes during implant surgery.

The content of this paper is organized as follows. In Section 2, we give a brief survey of related work. Section 3 expounds on our system architecture and methodology. In Section 4, we discuss the method and the results. A conclusion is given in Section 5.

2. RELATIVE WORK

Image segmentation is an important research area in image processing. It subdivides an image into its constituent regions or objects. The level to which the subdivision is carried depends on the problem being solved [1]. In the segmentation of medical images, several methods have been published in the literature. Many of them used pixel based segmentation approaches, such as thresholding and region growing.

Thresholding is a simple but effective filter to separate objects from the background [2]. In many applications of image processing, the gray levels of pixels belonging to the object are substantially different from the gray levels of the pixels belonging to the background. The output of thresholding operation is a binary image. The main problem with such technique is the choice of the threshold(s). Nobuyuki [3] and Wong [4] proposed the histogram thresholding method to use two or more thresholds based on the peaks and the valleys of the global histogram of an image. Do et al. [5] presented a fast and local thresholding algorithm which has the new feature with the circumscribed quadrangle on the segmented carotid artery for region of interest (ROI).

The region growing approach is one of the important image segmentation methods. The basic concept involves locally growing a "seed" to "annex" similar pixels into region and the quality of the segmentation is controlled by choosing a number of pixels, known as seeds as described in [6][7]. Muller et al. [8][9] proposed an evaluation function which combines the region growing and statistics that the range of a homogeneity threshold is deduced from the standard deviation of the initial seeds and their 3D-neighborhoods for the best segmentation corresponding to the optimal threshold. The use of arbitrary shaped ROIs can allow to spare non-negligible time which increases with algorithm complexity and data volume [10][11]. Pohle et al. [12][13] developed a region-based approach that learns its homogeneity criterion automatically from characteristics of the region to be segmented. This approach is less sensitive to the seed point location.

For successful implant surgery, it is crucial to locate internal structures such as the inferior alveolar nerve canal. Kress et al [14] found that it is possible to diagnose the interruption of nerve continuity by using MR imaging. Hanssen et al [15] needed to set two seed points and utilized geodesic active surfaces that are implemented with level sets for segmenting the nerve channels in the human mandible. Kondo et al [16] presented a computer-based method for extracting the inferior alveolar nerve canal by analyzing voxel intensities and discontinuities in 3-D gradient orientation in the panoramic images generated from the stack of raw CT images.

In this paper, the purpose is to segment the inferior alveolar nerve canal from 3D medical images for dental implant surgery. In Fig 2 we observe the cross sectional images which represent the cross-section of the alveolus can be segmented into the nerve canal more easily than original CT images. In order to obtain approximated cross sectional images of the nerve canal, we generate the dental arch curve and then build the cross sectional images which are perpendicular to CT images, as shown in Fig. 3(a). In the nerve canal extraction system (NCES), we propose an adaptive region growing method to segment the nerve canal. Dentists only need to select one initial seed point within the nerve canal region from cross sectional images and one end image to terminate our region growing method. The region growing method will adaptively segment the contour of the nerve canal and then automatically generate seed points in a series of images. Finally, the 3D nerve canal model can be acquired from the series of cross sectional images.

3. NERVE CANAL EXTRACTION SYSTEM

An overview of nerve canal extraction system (NCES) is given in Fig. 1. The first step is to input 3D medical images from dental CT device. The second step is to generate cross sectional image. A seed point is then selected from cross-section images to be the initial position in our adaptive region growing method. At the end, the 3D nerve canal can be rendered with the teeth model on the screen, as shown in Fig. 14. More details are described in the following sections.

3.1 Input Dental CT images

CT image is a thin section transverse to the patient's long axis. In the dental implant surgery, it is usually parallel to the occlusal plane, as shown in Fig. 2(a). The doctor can re-slice CT images in a different plane to display an anatomical structure in order to diagnose a large number of different disease entities. Thus the purpose of this paper is

to segment the nerve canal from the alveolus. We observe re-sliced images which are cross sectional images of the alveolus are clearer than CT images. Fig. 2 shows the contour of the nerve canal lies within the red circle region in different slice images. In order to obtain a good quality of the nerve canal, cross sectional images are the best choice to be input images of our adaptive region growing method.



Fig. 1: The flow chart of nerve canal extraction system.

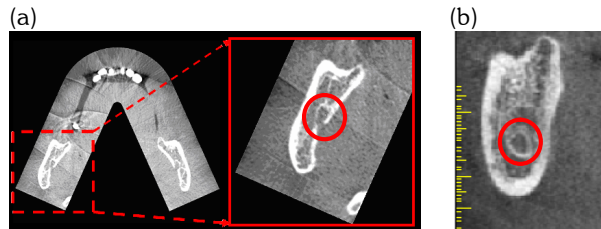


Fig. 2: The nerve canal region from different slice image. (a) Axial image. (b) Cross sectional image.

3.2 Building Cross Sectional Images

The cross sectional image is a thin and reformatted cross-section of the alveolus. At a first step to create cross sectional images, a dental arch should be generated. The dental arch is the curve that lies approximately in the middle of an axial slice of the jaw bone. In this paper, we select manually several points to fit a B-spline curve to express the dental arch. Therefore a set of points $\{Q_k\}$ are selected from a user, and interpolate these points with a p th-degree B-spline curve. The B-spline interpolation is the most widely used method [17]. If we assign a parameter value, \bar{u}_k , to each Q_k , and select an appropriate knot vector $U = \{u_0, \dots, u_m\}$, we can get the B-spline curve $C(u)$ from the following linear equations.

$$Q_k = C(\bar{u}_k) = \sum_{i=0}^n N_{i,p}(\bar{u}_k) P_i \tag{3.1}$$

where

P_i represent the control points that are the $n + 1$ unknowns and the parameter value \bar{u}_k was computed from Eqn. (3.2).

$$\begin{aligned} \bar{u}_k &= \bar{u}_{k-1} + \frac{|Q_k - Q_{k-1}|}{d} \quad k = 1, \dots, n-1 \\ \bar{u}_0 &= 0, \quad \bar{u}_n = 1 \end{aligned} \tag{3.2}$$

then

d is the total chord length, as follows :

$$d = \sum_{k=1}^n |Q_k - Q_{k-1}| \tag{3.3}$$

In Fig 3(a)., we illustrate all selected points and a dental arch which interpolates all selected points with red circles and a yellow curve. After the arch curve is established, the next step is to build the cross sectional lines (green lines), as shown in Fig 3(a). The slope of the cross section line is equal to the unit normal vector $\tilde{n}(u)$ of the dental arch. It can be calculated easily by using a tangent vector of the arch curve, as expressed as follows:

$$\tilde{n}(u) = \frac{(C'_y(u), -C'_x(u))}{\sqrt{C'_x(u)^2 + C'_y(u)^2}} \tag{3.4}$$

where

$C'(u) = (C'_x(u), C'_y(u))$ is the derivative of an arch curve.

Finally, the cross sectional images can be built by utilizing multi-planar reconstruction algorithm [18] to re-slicing CT images along the normal direction of the arch curve, as shown in Fig. 3(b).

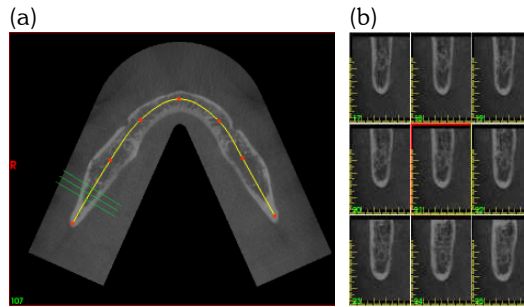


Fig. 3: Building cross sectional images from dental arch. (a) Arch curve (yellow) and section lines (green). (b) Cross sectional images.

3.3 Selecting Initial Seed Point

The region growing methods generally need a seed point and then from each seed point grows a region. The seed point is usually assigned by a user. Thus it can be seen that selecting seed points in all cross sectional images is very inconvenient and inefficient. However, it is difficult to automatically and exactly select all seed points in the region growing method. In order to deal with this problem, only one initial seed point needs be selected in our proposed system. Other seed points in each image can be automatically generated. The criterion to choose the initial seed point in practice is to select the center point of the nerve canal as near as possible. In addition to selecting the initial seed point, we also select one image to be our terminal image. This terminal image is to finish extracting the nerve canal by using adaptive region growing method.

3.4 Adaptive Region Growing Method

Our proposed adaptive region growing method consists of two important parts including nerve canal segmentation and seed point generation. Nerve canal segmentation is used to extract a contour of the nerve canal in current image and seed point generation is used to automatically build a seed point as an initial point for extracting a contour of the nerve canal in next image. Therefore our method can automatically and successively segment a nerve contour in each cross sectional image. Fig. 4 shows the flowchart of the adaptive region growing method and the details are described as follows:

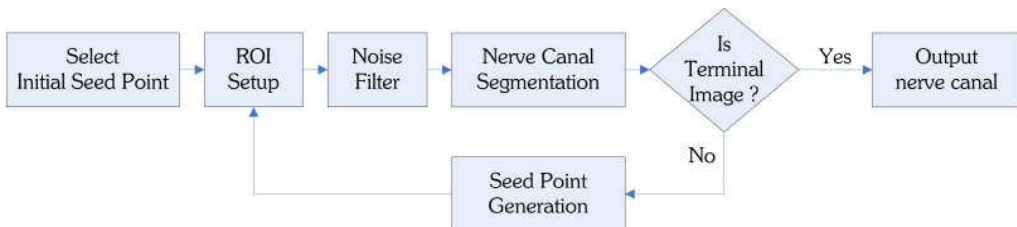


Fig. 4: Flowchart of the adaptive region growing method.

After the initial seed point is selected, we set a region of interesting (ROI) in the cross sectional image to avoid computing the unnecessary region without covering the contour of the nerve canal. In Fig. 5., a ROI in the cross sectional image is expressed as a green rectangular region and the center point of this ROI is a seed point. Then, the contour of the nerve canal in this ROI and a seed point in next cross sectional image will be automatically calculated by using nerve canal segmentation and seed point generation respectively. More details are described in Section 3.4.1 and Section 3.4.2. Finally, if the terminal image accomplished to extract a final contour of the nerve canal, the nerve canal model can be obtained from all series of nerve contours.

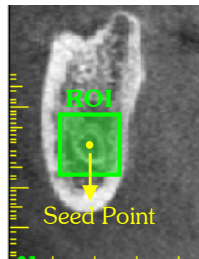


Fig. 5: A region of interesting in a cross sectional image.

3.4.1 Nerve Canal Segmentation

Nerve canal segmentation utilizes a region growing filter to extract a contour of nerve canal in each cross sectional image. This filter can be divided into two important steps as follows:

- The first step is to calculate characteristic values that are concerned with segmentation. The surroundings of the nerve canal are generally the bones, and the grayscale values within the nerve canal region are similar to the soft tissues. In order to get better characteristic values, we analyze the property of the nerve canal. In Fig. 6., the yellow circle is a seed point and we set it to be a center point. Then we observe the grayscale value distributions in x-direction and y-direction of this center point, as shown in Fig. 7(a). and Fig. 7(b). In these graphs, the horizontal axis denotes the position of the pixels and the vertical axis denotes the grayscale value. Obviously, the grayscale value distribution is like a shape of the valley in the nerve canal region and different region has different distribution. We will use this property to adaptively calculate the characteristic value as the growing thresholds in each cross sectional image and furthermore the nerve canal will be obtained more completely and accurately. Thus, the growing criterion is computed by using a statistical method. In this paper, the average of the grayscale values \bar{X} in the ROI can be calculated but the high grayscale values of the bone region may influence the mean value \bar{X} .

$$\bar{X} = \frac{1}{N} \sum_{i=1}^N x_i \quad x_i \in ROI \quad (3.5)$$

where N is the number of pixels in the ROI, and x_i is the grayscale value.

In order to decrease the effect, we re-compute the average of the grayscale values \bar{x} . If there are n pixels whose grayscale values are under the mean value \bar{X} , the sample mean value \bar{x} and its standard deviation σ are expressed as follows.

$$\bar{x} = \frac{1}{n} \sum_{i=1}^n x_i \quad x_i < \bar{X} \quad (3.6)$$

$$\sigma = \sqrt{\frac{1}{n} \sum_{i=1}^n (x_i - \bar{x})^2} \quad (3.7)$$

Therefore, the upper characteristic threshold is $\bar{x} + \sigma$ and the lower characteristic threshold is $\bar{x} - 2\sigma$.

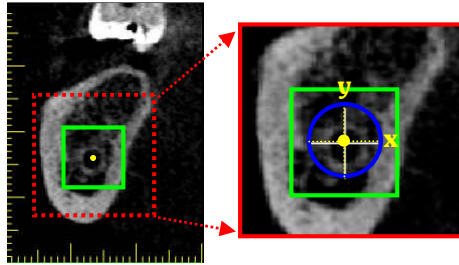


Fig. 6: Analysis of the property of the nerve canal.

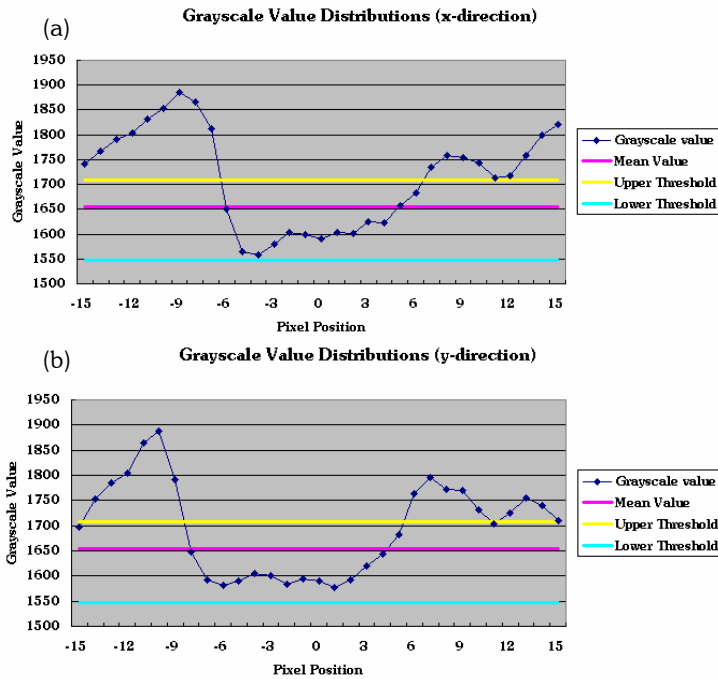


Fig. 7: The grayscale value distributions. (a) x-direction. (b) y-direction.

- The second step is to grow a region from a seed point, as shown in Fig. 8. The growing filter compares grayscale value with the eight neighborhoods of the seed point according to characteristic thresholds. If the grayscale value of the neighborhood is located within the upper and lower threshold, this neighborhood can be merged into the nerve region, else this neighborhood is rejected. This step is repeated from a pixel to another, till all the pixels in the image have been checked. Finally, the contour of the nerve canal region in the current image will be extracted.

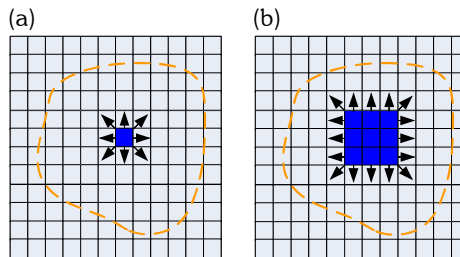


Fig. 8: The diagram of the region growing filter. (a) Initial state. (b) Expansion state.

3.4.2 Seed Point Generation

The threshold filter is a major method in our seed point generation. When pixels fall between a given lower and upper threshold, the threshold filter can extract these pixels. Accordingly, if the grayscale value of a pixel in the original image I is inside the given threshold, the grayscale value of this pixel in the threshold image I' will be set to one. Otherwise the other pixels will be zero.

$$I'(x,y) = \begin{cases} 1 & \text{if } T_{\min} < I(x,y) < T_{\max} \\ 0 & \text{else} \end{cases} \quad (3.9)$$

where T_{\max} and T_{\min} are the lower and upper threshold.

After obtaining a contour of the nerve canal region on current image, the new seed point on next image can be determined by using the threshold filter. The pipeline is explained as follows:

Fig. 9(a) shows the seed point and ROI on current image I with a contour of the nerve canal region. Fig. 9(b) shows the same ROI on next image I_{+1} and Fig. 9(c) shows the threshold image I'_{+1} which is generated by applying next image I_{+1} to Eqn. (3.9). Then an intersected region can be obtained from the current image I and the threshold image I'_{+1} , as shown in Fig. 9(d). Finally the center point of the intersected region will be a new seed point on the next image I_{+1} and the new ROI will also be reset simultaneously. Therefore, iteration with the region growing filtering and seed point generation continues from an image to another, until the terminal image has been checked. The final result of the nerve canal model can be obtained by lofting the successive contours.

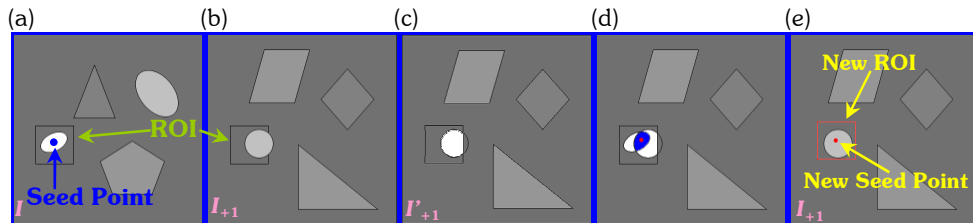


Fig. 9: The diagram of seed point generation. (a) The current image with a contour of the nerve canal region. (b) The next image. (c) The image result of the threshold filter (d) Intersected region. (e) New seed point and new ROI.

4. EXPERIMENTAL RESULTS AND DISCUSSION

In this section, we demonstrate one case to express all procedures in the NCES. In medical science, the dental arch consists of teeth on the edges of the maxillae. It includes the incisors, the canines, the premolars and the molars. In the NCES, the shape of the dental arch is generated by connection of manually selected points. It is a two-dimensional B-spline curve, as shown in Fig. 10.



Fig. 10: Dental arch curve generated by selecting points.

Traditionally, dentists usually examine their surgical plans in a panoramic x-ray image, as shown in Fig 11, and therefore the NCES can also utilize the dental arch and the original CT images to create approximated panoramic images, as shown in Fig 12.

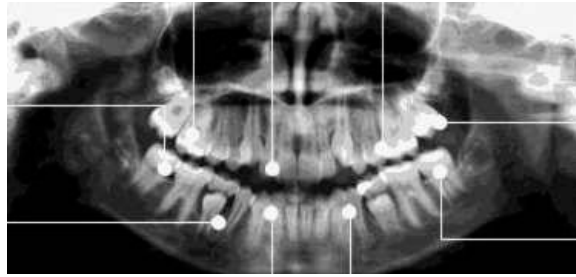


Fig. 11: Panoramic x-ray image [19].



Fig. 12: Panoramic image.

The cross sectional images are generated by re-slicing CT images along the normal direction of the arch curve, as shown in Fig. 13.

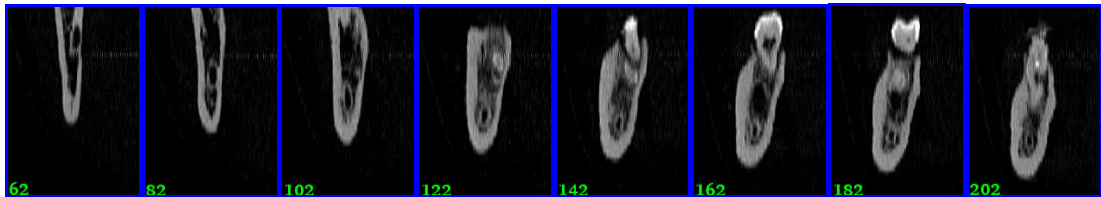


Fig. 13: Cross sectional images.

The user must select only one initial seed point on the first cross sectional image and one terminal image in our proposed system. Then the all contours of the nerve canal and all seed points will be automatically generated without any user defined parameter and operation, as shown in Fig. 14.

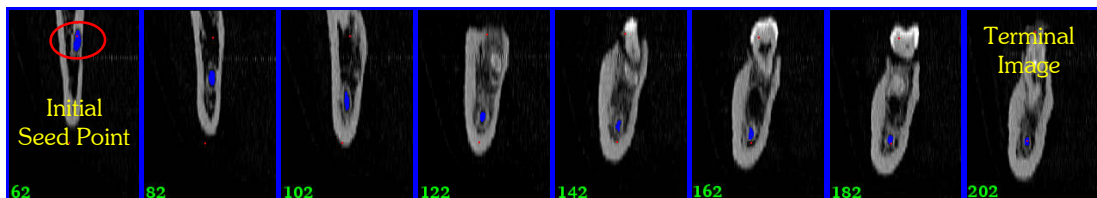


Fig. 14: Adaptive region growing method--Contours of the nerve canal and seed points.

Finally, the mesh constructed from all contours of the nerve canal contrasted with the original mandible model and they are both drawn on the screen, as shown in Fig 15. If the implant model also shows on the screen, dentists can easily and conveniently observe the relation between the implant fixtures and the nerve canal. Thus, the NCES can help dentists avoid mistakes in the preoperative planning.

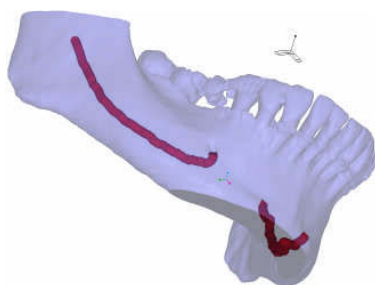


Fig. 15: Nerve canal model and mandible model.

4.1 Efficiency and Accuracy

The proposed method has been implemented in C++ and some test cases were run on a 1.86GHz Intel Core 2 Duo E6300 computer. Tab. 1 gives a comparison of computation time in two different cases.

In commercial implant software, the nerve canal is drawn manually and consists of a series of points, connected by an interpolated line. These methods need more time to extract the alveolar nerve, but in our NCES, the user only selects one initial seed point and one terminal image to generate the nerve. The extraction of the nerve canal has become more convenient. In addition, our algorithm adaptively sets the ROI in all images to decrease computation time so our proposed method is very efficient. Moreover, our algorithm also automatically generates seed points and adaptively calculates the characteristic value to obtain more complete and accurate nerve model.

	Original Image	Cross Sectional Image	Time(sec)
	512×512×44 (0.3×0.3×1.0 mm)	151×216×400	10
	900×800×266 (0.15×0.15×0.15 mm)	151×199×400	9

Tab. 1: Computation time.

5. CONCLUSION

The objective of this paper is to segment the inferior alveolar nerve canal in CT images. The nerve canal extraction system (NCES) can help dentists find the nerve canal before implant surgery, thereby reducing the risk of injury to patients. In summary, the advantages of this NCES presented in this paper are as follows:

- The conventional method for segmenting nerve canal usually needs to assign the seed points in all CT images. In the NCES, we just select one initial seed point and the other seed points are generated automatically. This can simplify the segmentation process.
- During the region growing process, our algorithm can adaptively adjust the minimum and maximum grayscale values as the growing criteria. We use a statistical method to analyze the property of the nerve canal in all medical images. Thus, the NCES is robust and reliable.
- In some medical images, the contour of the nerve canal is not a closed region. This will cause the segmented region to make some mistakes. In this paper, the ROI can also be used as the boundary conditions to solve this problem.

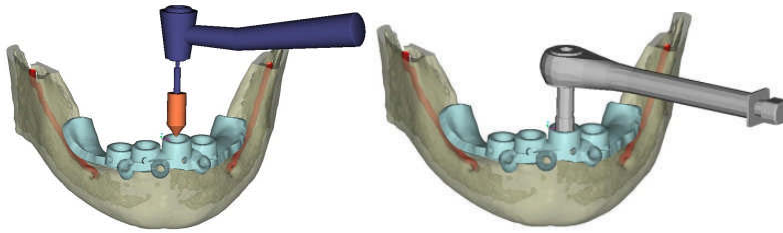


Fig. 14: Dental implant surgical simulation.

In our future work, the nerve canal model will be applied to dental implant surgical simulation. This simulation combines the virtual reality and haptic device, as shown in Fig. 14. The dentist can use this system as a training tool before implant surgery.

6. REFERENCES

- [1] Gonzalez R. C.; Woods R. E.: *Digital Image Processing*, Prentice Hall, 2002.
- [2] Sezgin, M.; Sankur, B.: Survey over image thresholding techniques and quantitative performance evaluation, *Journal of Electronic Imaging*, 13(1), 2004, 146-168.
- [3] Nobuyuki O.: A Threshold Selection Method from Gray-Level Histograms, *Journal of IEEE Transactions on Systems*, 9(1), 1979, 62-66.
- [4] Wong, A. K. C.; Sahoo, P. K.: A gray-level threshold selection method based on maximum entropy principle, *IEEE Transactions on Systems, Man, and Cybernetics*, 19(4), 1989, 866-871.
- [5] Do, Y. K.; Jong, W. P.: Connectivity-based local adaptive thresholding for carotid artery segmentation using MRA images, *Image and Vision Computing*, 23(14), 2005, 1277-1287.
- [6] Pardo, X. M.; Carreira, M. J.; Mosquera, A.; Cabello, D.: A snake for CT image segmentation integrating region and edge information, *Image and Vision Computing*, 19(7), 2001, 461-475.
- [7] Adams, R.; Bischof, L.: Seeded region growing, *Transactions on Pattern Analysis and Machine Intelligence*, 16(6), 1994, 641-647.
- [8] Muller, C. R.; Cattin, H. B.; Carillon, Y.; Odet, C.; Briguët, A.; Peyrin, F.: Bone MRI Segmentation Assessment Based, *IEEE Transactions on Nuclear Science*, 49(1), 2002, 220-224.
- [9] Muller, C. R.; Peyrin, F.; Odet, C.; Carillon, Y.: Automated 3D region growing algorithm governed by an evaluation function, *International Conference on Image Processing*, 3, 2000, 440-443.
- [10] Fasquel, J.; Agnus, V.; Moreau, J.; Soler, L.; Marescaux, J.: An interactive medical image segmentation system based on the optimal management of regions of interest using topological medical knowledge, *Computer Methods and Programs in Biomedicine*, 82(3), 2006, 216-230.
- [11] Fasquel, J.; Agnus, V.; Lamy, J.: An efficient and generic extension to ITK to process arbitrary shaped regions of interest, *computer methods and programs in biomedicine*, *Computer Methods and Programs in Biomedicine*, 81(1), 2006, 1-7.
- [12] Pohle, R.; Toennies, K. D.: A new approach for model-based adaptive region growing in medical image analysis, *Computer Analysis of Images and Patterns: 9th International Conference*, 2124, 2001, 238-246.
- [13] Pohle, R.; Toennies, K. D.: Segmentation of medical images using adaptive region growing, *SPIE Medical Imaging*, 4322, 2001, 1337-1346.
- [14] Kress, B.; Gottschalk, A.; Stippich, C.; Palm, F.; Bähren, W.; Sartor K.: MR Imaging of Traumatic Lesions of the Inferior Alveolar Nerve in Patients with Fractures of the Mandible, *American Journal of Neuroradiology*, 24, 1635-1638.
- [15] Hanssen, N.; Burgielski, Z.; Jansen, T.; Lievin, M.; Ritter, L.; von Rymon-Lipinski, B.; Keeve, E.: Nerves - level sets for interactive 3D segmentation of nerve channels, 1, 2004, 201-204.
- [16] Kondo, T.; Ong, S.; Foong, K.: Computer-based extraction of the inferior alveolar nerve canal in 3-D space, *Computer Methods and Programs in Biomedicine*, 76(3), 2004, 181-191.
- [17] Piegl, L.; Tiller, W.: *The NURBS Book*, Springer, New York, 1997.
- [18] David, P.; Naidich, M. D.: *Computed Tomography and Magnetic Resonance of the Thorax*, Raven, New York, 1991.
- [19] Panoramic x-ray image, <http://www.radtechxray.com/serv02.htm>.